REPORT DOCUMENTATION PAGE

Form Approved OMB NO. 0704-0188

1. REPORT DATE (DD-MM-YYYY)	2. REPORT TYPE	3. DATES COVERED (From - To)
11-01-2017	Final Report	1-Nov-2010 - 30-Sep-2016

4. TITLE AND SUBTITLE
Final Report: Development, Modeling and Test of Optical Coatings with Novel Thermal and Stress Management for High Energy Laser Applications

5a. CONTRACT NUMBER
W911NF-11-1-0007

5b. GRANT NUMBER

5c. PROGRAM ELEMENT NUMBER
611102

6. AUTHORS
Wolfgang Rudolph, Luke Emmert, Carmen Menoni

5d. PROJECT NUMBER

5e. TASK NUMBER

5f. WORK UNIT NUMBER

7. PERFORMING ORGANIZATION NAMES AND ADDRESSES
University of New Mexico Albuquerque
1700 Lomas Blvd. NE, Suite 2200, MSC01 1247
1 University of New Mexico
Albuquerque, NM 87131 -0001

8. PERFORMING ORGANIZATION REPORT NUMBER

9. SPONSORING/MONITORING AGENCY NAME(S) AND ADDRESS (ES)
U.S. Army Research Office
P.O. Box 12211
Research Triangle Park, NC 27709-2211

10. SPONSOR/MONITOR'S ACRONYM(S)
ARO

11. SPONSOR/MONITOR'S REPORT NUMBER(S)
58499-EL-HEL.42

12. DISTRIBUTION AVAILIBILITY STATEMENT
Approved for Public Release; Distribution Unlimited

13. SUPPLEMENTARY NOTES
The views, opinions and/or findings contained in this report are those of the author(s) and should not contrued as an official Department of the Army position, policy or decision, unless so designated by other documentation.

14. ABSTRACT
The purpose of this multiyear collaboration between groups at the University of New Mexico and Colorado State University was to improve our understanding of optical coatings used in high average power (CW and long-pulse) laser systems. While laser-induced damage by subpicosecond pulses has been studied extensively, damage mechanisms by high power CW and nanosecond (ns) and longer pulse laser sources have been little studied. What is known, is that damage results from as-yet undetected defects in the optical coatings. The goal of this project was to understand and to mitigate the defects in the coating that lead to damage under laser irradiation. In this final

15. SUBJECT TERMS
high energy lasers, optical coatings, thermal damage, third harmonic microscopy

16. SECURITY CLASSIFICATION OF:			17. LIMITATION OF ABSTRACT	15. NUMBER OF PAGES	19a. NAME OF RESPONSIBLE PERSON
a. REPORT	b. ABSTRACT	c. THIS PAGE			Wolfgang Rudolph
UU	UU	UU	UU		19b. TELEPHONE NUMBER 505-277-2616

Report Title

Final Report: Development, Modeling and Test of Optical Coatings with Novel Thermal and Stress Management for High Energy Laser Applications

ABSTRACT

The purpose of this multiyear collaboration between groups at the University of New Mexico and Colorado State University was to improve our understanding of optical coatings used in high average power (CW and long-pulse) laser systems. While laser-induced damage by subpicosecond pulses has been studied extensively, damage mechanisms by high power CW and nanosecond (ns) and longer pulse laser sources have been little studied. What is known, is that damage results from as-yet undetected defects in the optical coatings. The goal of this project was to understand and to mitigate the defects in the coating that lead to damage under laser irradiation. In this final report we list the accomplishments of this project and highlight the following four activities: (1) Study of defects in ion-beam sputtered Sc2O3 films; (2) Increased laser damage resistance of multilayer mirrors by modification of the top layer design; (3) The development of a single-pulse damage testing protocol (STEREO-LID) that is superior to the ISO standard for characterizing defects in films; and (4) Third harmonic generation in optical coatings for microscopy of defects and UV pulse generation.

Enter List of papers submitted or published that acknowledge ARO support from the start of the project to the date of this printing. List the papers, including journal references, in the following categories:

(a) Papers published in peer-reviewed journals (N/A for none)

Received	Paper
08/30/2014 11.00	P. F. Langston, E. Krous, D. Schiltz, D. Patel, L. Emmert, A. Markosyan, B. Reagan, K. Wernsing, Y. Xu, Z. Sun, R. Route, M. M. Fejer, J. J. Rocca, W. Rudolph, C. S. Menoni. Point defects in Sc_2O_3 thin films by ion beam sputtering, Applied Optics, (01 2014): 0. doi: 10.1364/AO.53.00A276
08/30/2014 12.00	Xuerong Zhang, Luke A. Emmert, Wolfgang Rudolph. Time-dependent absorption of TiO_2 optical thin films under pulsed and continuous wave 790??nm laser irradiation, Applied Optics, (11 2013): 0. doi: 10.1364/AO.52.008245
08/31/2014 19.00	Reed A. Weber, Cristina Rodriguez, Duy N. Nguyen, Luke A. Emmert, Dinesh Patel, Carmen S. Menoni, Wolfgang Rudolph. Third harmonic microscopy of intrinsic and induced material anisotropy in dielectric thin films, Optical Engineering, (12 2012): 121807. doi:
08/31/2015 20.00	Matthias Lenzner, Wolfgang Rudolph, Zhanliang Sun. Generic incubation law for laser damage and ablation thresholds, Journal of Applied Physics, (02 2015): 73102. doi: 10.1063/1.4913282
08/31/2015 21.00	Cristina Rodríguez, Wolfgang Rudolph. Characterization and Chi^3 measurements of thin films by third-harmonic microscopy, Optics Letters, (10 2014): 6042. doi: 10.1364/OL.39.006042
08/31/2015 22.00	Wolfgang Rudolph, Cristina Rodríguez. Modeling third-harmonic generation from layered materials using nonlinear optical matrices, Optics Express, (10 2014): 25984. doi: 10.1364/OE.22.025984
08/31/2015 23.00	Yejia Xu, Wolfgang Rudolph, Luke A. Emmert. Determination of defect densities from spatiotemporally resolved optical-laser induced damage measurements, Applied Optics, (07 2015): 6813. doi: 10.1364/AO.54.006813
08/31/2015 24.00	Wolfgang Rudolph, Luke A. Emmert, Yejia Xu. Spatio-TEmporally REsolved Optical Laser Induced Damage (STEREO LID) technique for material characterization, Optics Express, (08 2015): 21607. doi: 10.1364/OE.23.021607
TOTAL:	**8**

Number of Papers published in peer-reviewed journals:

(b) Papers published in non-peer-reviewed journals (N/A for none)

Received Paper

TOTAL:

Number of Papers published in non peer-reviewed journals:

(c) Presentations

Number of Presentations: 0.00

Non Peer-Reviewed Conference Proceeding publications (other than abstracts):

Received		Paper
01/04/2017	34.00	Christian Karras, Zhanliang Sun, Duy Nguyen, Luke Emmert, Wolfgang Rudolph. The impact ionization coefficient in dielectric materials revisited, XLIII Annual Symposium on Optical Materials for High Power Lasers. 18-SEP-11, Boulder, Colorado. : ,
01/04/2017	39.00	Luke Emmert, Cristina Rodriguez, Zhanliang Sun, Farzin Beygi Azar Aghbolagh, Stefan Guenster, Detlev Ristau, Dinesh Patel, Carmen Menoni, Wolfgang Rudolph. Optical coatings excited by femtosecond lasers near the damage threshold: challenges and opportunities, SPIE Laser Damage. 27-SEP-15, Boulder, Colorado, United States. : ,
01/04/2017	38.00	Yejia Xu, Amir Khabbazi, Travis Day, Andrew Brown, Luke Emmert, Joseph Talghader, Ella Field, Damon Kletecka, John Bellum, Dinesh Patel, Carmen Menoni, Wolfgang Rudolph. Comparative STEREO-LID (Spatio-TEmporally REsolved Optical Laser-Induced Damage) studies of critical defect distributions in IBS, ALD, and electron-beam coated dielectric films, SPIE Laser Damage. 27-SEP-15, Boulder, Colorado, United States. : ,
01/04/2017	37.00	Matthias Lenzner, Zhanliang Sun, Wolfgang Rudolph. Determination of multi-pulse damage thresholds from crater size measurements, Laser-Induced Damage in Optical Materials: 2014. 14-SEP-14, Boulder, Colorado, United States. : ,
01/10/2017	13.00	Wolfgang Rudolph, Luke Emmert, Zhanliang Sun, Dinesh Patel, Carmen Menoni. Laser damage in dielectric films: What we know and what we don't, SPIE Laser Damage. 22-SEP-13, Boulder, Colorado, USA. : ,
01/10/2017	15.00	Zhanliang Sun, Luke Emmert, Xuerong Zhang, Ahmad Mansoori, Dinesh Patel, Carmen Menoni, Wolfgang Rudolph. Confocal photothermal microscopy of thin films based on etalon and thermal lensing effects, SPIE Laser Damage. 22-SEP-13, Boulder, Colorado, USA. : ,
01/10/2017	1.00	Wolfgang Rudolph, Luke Emmert, Duy Nguyen, Christian Karras, Zhanliang Sun, Reed Weber. Subpicosecond laser breakdown in optical thin films, Pacific Rim Laser Damage 2011: Optical Materials for High Power Lasers. 06-NOV-11, Shanghai, China. : ,
01/10/2017	2.00	Reed Weber, Cristina Rodriguez, Duy Nguyen, Luke Emmert, Wolfgang Rudolph, Dinesh Patel, Carmen Menoni. Third harmonic microscopy for optical material characterization, Laser-Induced Damage in Optical Materials: 2011. 18-SEP-11, Boulder, Colorado, USA. : ,
TOTAL:		**8**

Number of Non Peer-Reviewed Conference Proceeding publications (other than abstracts):

Peer-Reviewed Conference Proceeding publications (other than abstracts):

Received		Paper
01/10/2017	6.00	Carmen Menoni, Peter Langston, Erik Krous, Dinesh Patel, Luke Emmert, Ashot Markosyan, B. Reagan, K. Wernsing, Yejia Xu, Zhanliang Sun, Roger Route, Martin Fejer, Jorge Rocca, Wolfgang Rudolph. What role do defects play in the laser damage behavior of metal oxides?, SPIE Laser Damage. 23-SEP-12, Boulder, Colorado, USA. : ,
01/10/2017	8.00	Wolfgang Rudolph, Luke Emmert, Cristina Rodriguez, Zhanliang Sun, Xuerong Zhang, Yejia Xu. Femtosecond to nanosecond laser damage in dielectric materials, SPIE/SIOM Pacific Rim Laser Damage: Optical Materials for High-Power Lasers. 19-MAY-13, Shanghai, P. R. China. : ,
01/10/2017	9.00	Dinesh Patel, Peter Langston, L. Imbler, Luke Emmert, Ashot Markosyan, Roger Route, Martin Fejer, Wolfgang Rudolph, Carmen Menoni. Ion beam sputtered Y₂O<sub>3< /sub>, SPIE Laser Damage. 23-SEP-12, Boulder, Colorado, USA. : ,
01/10/2017	25.00	Drew Schiltz, Dinesh Patel, Luke Emmert, C Baumgarten, B Reagan, Wolfgang Rudolph, Jorge Rocca, Carmen Menoni. Modification of multilayer mirror top-layer design for increased laser damage resistance, SPIE Laser Damage. 14-SEP-14, Boulder, Colorado, United States. : ,
TOTAL:	**4**	

Number of Peer-Reviewed Conference Proceeding publications (other than abstracts):

(d) Manuscripts

Received		Paper
TOTAL:		

Number of Manuscripts:

Books

Received Book

TOTAL:

Received Book Chapter

TOTAL:

Patents Submitted

Harmonic generation using optimized stacks of thin films

Patents Awarded

Awards

1. Best Poster Award at SPIE Laser Damage Symposium in 2011 for Cristian Karras et al. "The impact ionization coefficient in dielectric materials revisited"

2. Best Presentation Award at SPIE Laser Damage Symposium in 2012 for Carmen Menoni et al. "What role do point defects play in the laser damage behavior of metal oxides"

Graduate Students

NAME	PERCENT_SUPPORTED	Discipline
Amir Khabbazi Oskouei	0.12	
Zhanliang Sun	0.23	
Ahmad Mansoori	0.17	
Rhett Eller	0.04	
Yejia Xu	0.48	
Behshad Roshanzadeh	0.12	
Cristina Rodriguez	0.17	
Xuerong Zhang	0.20	
Drew Schiltz	0.00	
Travis Day	0.06	
Tyler Green	0.10	
Emmet Randel	0.06	
Le Yang	0.03	
Reed Weber	0.00	
FTE Equivalent:	**1.78**	
Total Number:	**14**	

Names of Post Doctorates

NAME	PERCENT_SUPPORTED
Fabio DeMoraes Cavalcante	0.10
FTE Equivalent:	**0.10**
Total Number:	**1**

Names of Faculty Supported

NAME	PERCENT_SUPPORTED	National Academy Member
Luke Emmert	0.83	
Wolfgang Rudolph	0.08	
Carmen Menoni	0.10	
FTE Equivalent:	**1.01**	
Total Number:	**3**	

Names of Under Graduate students supported

NAME	PERCENT_SUPPORTED	Discipline
Jeremy Rencher	0.00	Electrical and Computer Engineering
Matthew Carter	0.02	Biomedical Engineering
Lang Simmons	0.01	Physics
FTE Equivalent:	**0.03**	
Total Number:	**3**	

Student Metrics

This section only applies to graduating undergraduates supported by this agreement in this reporting period

The number of undergraduates funded by this agreement who graduated during this period:	0.00
The number of undergraduates funded by this agreement who graduated during this period with a degree in science, mathematics, engineering, or technology fields:.....	0.00
The number of undergraduates funded by your agreement who graduated during this period and will continue to pursue a graduate or Ph.D. degree in science, mathematics, engineering, or technology fields:.....	0.00
Number of graduating undergraduates who achieved a 3.5 GPA to 4.0 (4.0 max scale):.....	0.00
Number of graduating undergraduates funded by a DoD funded Center of Excellence grant for Education, Research and Engineering:.....	0.00
The number of undergraduates funded by your agreement who graduated during this period and intend to work for the Department of Defense	0.00
The number of undergraduates funded by your agreement who graduated during this period and will receive scholarships or fellowships for further studies in science, mathematics, engineering or technology fields:	0.00

Names of Personnel receiving masters degrees

NAME
Xuerong Zhang
Total Number: **1**

Names of personnel receiving PHDs

NAME
Reed Weber
Cristina Rodriguez
Zhanliang Sun
Total Number: **3**

Names of other research staff

NAME	PERCENT_SUPPORTED
Dinesh Patel	0.20
Brendan Reagan	0.02
Elzbieta Jankowska	0.17
FTE Equivalent:	**0.39**
Total Number:	**3**

Sub Contractors (DD882)

Inventions (DD882)

5 **Harmonic generation of laser radiation using optimized stacks of thin films**

Patent Filed in US? (5d-1) Y

Patent Filed in Foreign Countries? (5d-2) N

Was the assignment forwarded to the contracting officer? (5e) N

Foreign Countries of application (5g-2):

5a: Cristina Rodriguez

5f-1a: University of New Mexico

5f-c: 1919 Lomas Blvd NE

Albuquerque NM 87131

5a: Wolfgang Rudolph

5f-1a: University of New Mexico

5f-c: 1919 Lomas Blvd NE

Albuquerque NM 87131

Scientific Progress

Technology Transfer

Final Report: Development, Modeling and Test of Optical Coatings with Novel Thermal and Stress Management for High Energy Laser Applications

Final Report
November 1, 2010 -- September 30, 2016

Luke A. Emmert and Wolfgang Rudolph
Dept. of Physics and Astronomy, University of New Mexico

Carmen S. Menoni
Dept. of Electrical and Computer Engineering, Colorado State University

Table of Contents

List of Figures

Statement of Problem

The purpose of this multiyear project has been to improve our understanding of optical coatings used in high average power (CW and long-pulse) laser systems. While pulsed-laser damage has been studied extensively, only recently have models of laser-matter interaction been able to explain the damage behavior, in particular for picosecond (ps) and shorter pulse durations. Laser-material interactions involving high power CW and nanosecond (ns) and longer pulse laser sources, where thermal effects are more important, had been little studied.

This project was focused on optical coatings prepared by ion-beam sputtering (IBS), but the findings on laser-matter interactions leading to damage and optical performance deterioration are generally applicable. IBS produces coatings which are nearly amorphous, close to bulk density, and environmentally robust. These are ideal qualities for optical coatings.

The components of this project have been broken down in three topics: (1) Novel Functional Materials and Optical Stack Design; (2) Modeling; and (3) Testing and Diagnostics Development. The significant achievements were published. They are:

Novel Functional Materials and Optical Stack Design:

1. Study of defects in ion-beam sputtered Sc_2O_3 films [1,2,3].
2. Optimization of ion-beam sputtered Y_2O_3 film deposition conditions [4].
3. Advanced mirror designs by manipulation of the top layers [5,6,7].
4. Demonstration of nonlinear optics (third harmonic generation) [8].

Modeling:

1. Thermal modeling and measurement of thermal conductivity of IBS coatings.
2. Generic incubation model [9].
3. Modeling of intrinsic damage mechanism by long pulses [1].

Testing and Diagnostics Development:

1. Development of microscopes for absorption and scatter characterization [10].
2. Measurement of laser-induced absorption in Ta_2O_5 and TiO_2 [11].
3. Development of wavefront measurement for detecting bending of thick substrates by coatings [12].
4. Development of third harmonic microscope for identifying defects in amorphous coatings [13].
5. Testing of high-reflector coatings at Air Force Research Laboratory at Kirtland AFB.
6. Development of novel single-pulse damage testing protocol (STEREO-LID) for characterization of defects in optical coatings and surfaces [14,15,16,17].

Details of the accomplishments are provided in the references and/or previous (annual) reports. In this final report the following major accomplishments are highlighted:

1. Study of defects in ion-beam sputtered Sc_2O_3 films.
2. Increased laser damage resistance of multilayer mirrors by modification of the top layer design.

3. The development of a single-pulse damage testing protocol (STEREO-LID) and its characterization of defect densities in high index coatings and the initial kinetics of laser-induced damage.
4. Third harmonic generation in optical coatings: characterization of defects and frequency conversion in thin films and stacks.

Research Highlights

1. Study of point defects in ion-beam sputtered Sc_2O_3 films

The goal of this work was to study the effect of key deposition parameters on the optical and structural/mechanical properties of oxide coatings. The material selected was Sc_2O_3 because it is a promising material for pulsed-laser applications and has been little studied in comparison to other materials. However, the results should be applicable to most of the metal oxides. The deposition technique used was ion-beam sputtering (IBS) where material from a metal (Sc) target is sputtered by an argon ion beam and reacts on the substrate surface with oxygen (O_2) introduced as a background gas. The deposition parameters studied were the accelerating voltage of the argon beam and the flow rate (relates to pressure) of the oxygen supply. The resulting films were studied by absorption measurements, x-ray photoelectron spectroscopy (XPS, provides chemical information), electron-spin resonance (ESR, sensitive to some point defects), x-ray diffraction (XRD), and stress measurements.

Figure 1 shows the results for absorption measurements at λ=1.064 µm. The absorption increases with increasing oxygen partial pressure and with increasing beam voltage.

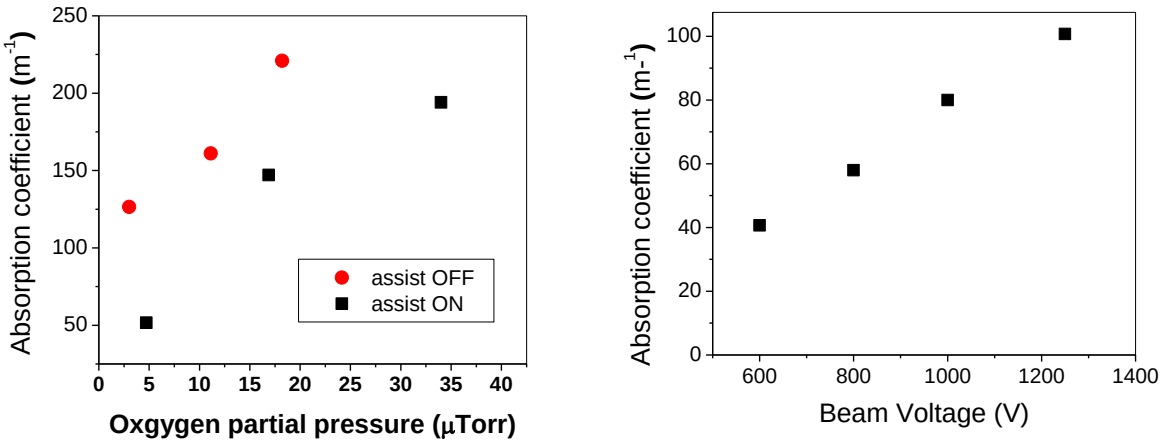

(a) (b)

Figure 1: Absorption coefficient (at λ=1.064 µm) vs. (a) oxygen partial pressure and (b) beam voltage. The assist beam in (a) refers to a second ion beam that improves mobility on the growth film surface.

Figures 2a and 2b show the result of XPS and EPR measurements. The XPS result indicates the presence of oxygen in a different chemical environment then the bulk of the oxygen in the film.

The EPR data show the presence of O_2^- ions within the film. These findings are consistent with the presence of interstitial oxygen in the film.

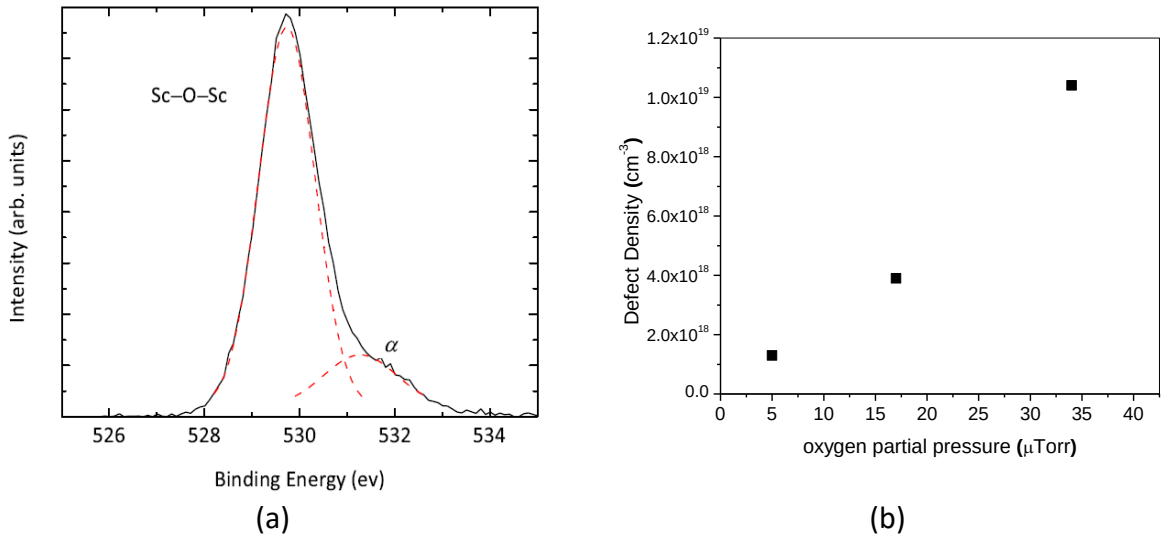

Figure 2: (a) A typical XPS O 1s peak from Sc_2O_3. The side peak at lower binding energy, labeled α, indicates the presence of oxygen with a difference chemical environment than the bulk of the material. (b) The density of O_2^- complexes (from EPR measurements) within the film as a function of the oxygen partial pressure.

Figures 3a and 3b show the stress and shift of the (222) diffraction peak as a function of oxygen partial pressure, respectively. These indicate that the film is under increasing internal stress with increasing oxygen flow during deposition.

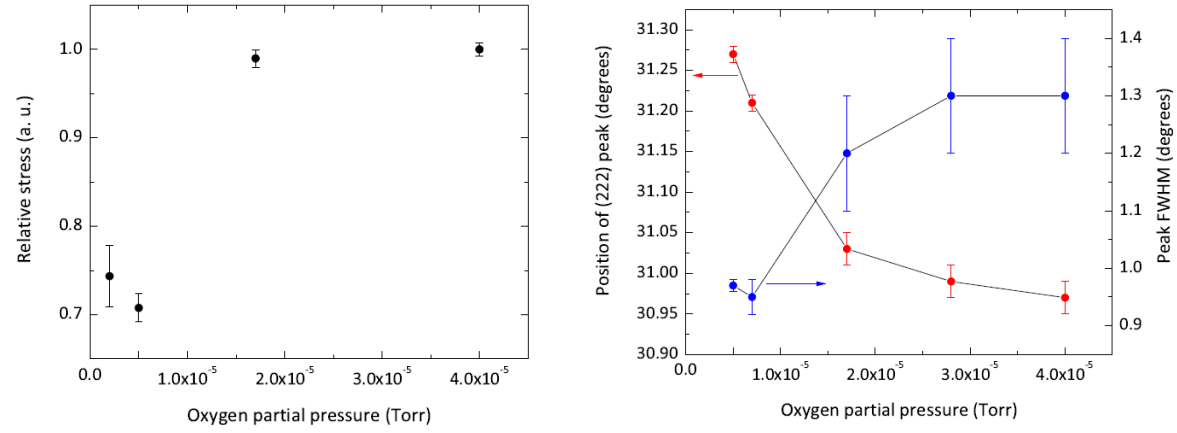

Figure 3: (a) The stress vs. oxygen partial pressure during IBS of a Sc_2O_3 film . (b) Position and width (FWHM) of the (222) diffraction peak vs. oxygen partial pressure.

The result of all these measurements is that increasing the oxygen pressure (flow) during deposition leads to an excess of oxygen within the films that is incorporated as oxygen interstitial defects. These defects lead to internal stress within the films and create electronic

states that can provide additional absorption channels. These states have been predicted in the literature through theoretical calculations [18]. Similar results were shown for the effect of the beam voltage. The conclusion from these studies is that there should be just enough oxygen to produce a fully stoichiometric film and that any excess will degrade the film properties. These results should be true in general for any metal oxide, not just SC_2O_3.

2. Increased laser damage resistance of multilayer mirrors by modification of the top layer design

Ta_2O_5 is a prime candidate for a high index material in interference coatings given its low intrinsic stress superior layer smoothness and uniformity and low absorption and scattering losses. Its laser damage resistance for nanosecond pulse durations is, however, lower than similar multilayers that incorporate HfO_2 or Y_2O_5 as the high index material.

We have already demonstrated a 50 % increase in the laser damage threshold of a Ta_2O_5/SiO_2 high reflection multilayer through replacement of Ta_2O_5 with HfO_2 in the top three bilayers when tested using 350 ps pulses at λ = 1 μm [5]. We have shown that by modifying the design of the top few layers it is possible to increase the damage resistance of Ta_2O_5/SiO_2 high reflectors by almost 100% as shown in Fig. 4 [6,7].

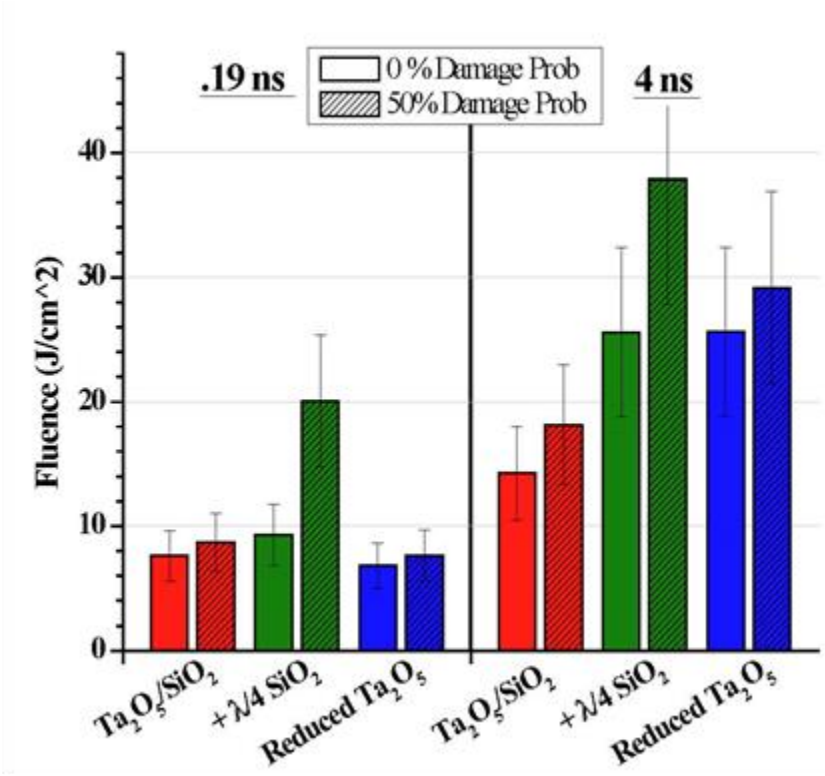

Figure 4: 50% probability laser damage fluence determined from 100-on-1 tests on Ta_2O_5/SiO_2 quarter wave stacks.

3. STEREO-LID: Spatially-TEmporally REsolved Laser-Induced Damage

3.1. Description of the technique

The traditional method for measuring the laser-induced damage threshold of optical materials only records whether or not damage occurs during a single test and relies on statistics of repeated tests to extrapolate a damage threshold. A single-shot measurement, which records the actual threshold in a single test, is more efficient and can be used in conjunction with non-destructive tests to identify the critical defects responsible for laser-induced damage in optical materials. A new technique dubbed STEREO-LID for Spatially-TEmporally REsolved Laser-Induced Damage was developed for this reason [14]. It is so named because the technique identifies the time and location of damage initiation within a pulse shape and beam profile in order to retrieve the local intensity and accumulated fluence at the onset of damage.

Given the damage initiation time, t_d, and the damage initiation position, (x_d, y_d), the threshold fluence of the defect responsible can be calculated using

$$F_{th} = \int_0^{t_d} I_0(t)\, e^{-\left(\frac{{x_d}^2}{2{w_x}^2}+\frac{{y_d}^2}{2{w_y}^2}\right)} \quad (1)$$

where $I_0(t)$ is the peak intensity as a function of time, as provided by a reference photodiode, and w_x and w_y are the characterize the size of the beam. The threshold intensity can be calculated in a similar manner.

The layout of the experimental setup is shown in Fig. 5. Damage is initiated by the dielectric breakdown and plasma formation around a defect. The time of damage initiation is determined by either a change in scatter or transmission that results from dielectric breakdown. The location of damage is identified by imaging light scattering off a localized ablation jet using an in situ microscope (CCD1). These two bits of information (time and space) along with a calibrated reference diode allow for the measurement of the LIDT with a single test.

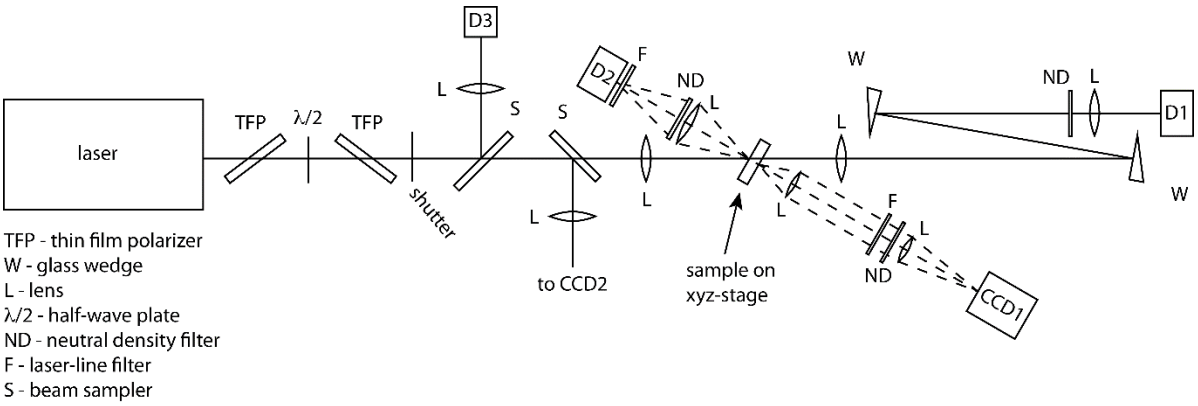

(a)

(b)

Figure 5: (a) Experimental layout of single-shot damage test station. (b) Photograph of its implementation.

3.2. Characterization of defect densities in high index films

An important role of damage testing is to characterize defect densities in optical materials. This provides feedback to adjust deposition conditions for coatings. The defect ensemble of an optic can be described by a defect distribution function where $\bar{\rho}(F)dF$ is the density of defects with a threshold fluence in the range from F to $F + dF$. While the traditional damage test (TDT) is often used to measure a defect density, the best that it can provide is often a crude picture of an average defect density, ρ_0, that will fail at a single fluence F_{th}. Because STEREO-LID probes individual defects, it can provide a more complete picture of defect densities.

Repeated measurements using the STEREO-LID method produces the probability of exciting a defect $P(F)$. (It actually produces a discrete set of probability $P_i = P(F_i)$ where F_i is a set of fluence bins into which the measured damage fluences are counted.) Through counting statistics [15], these probabilities can be used to retrieve the defect density distribution through the following equation:

$$P_i = \sum_{n=0}^{M-i-1} \left\{ \frac{\rho_i}{\rho_{T,i+n}} \prod_{j=1}^{i+n} \left(\frac{F_j}{F_i}\right)^{s\rho_j} \times \left[\left(\frac{F_i}{F_{i+n}}\right)^{s\rho_{T,i+n}} + \left(\frac{F_i}{F_{i+n+1}}\right)^{s\rho_{T,i+n}} \right] \right\}. \quad (2)$$

Where M is the number of fluence bins, ρ_i is the density of defects with damage fluence F_i, ρ_T is the total density of defects, and s is the area of the test beam.

To demonstrate the power of STEREO-LID in characterizing films, two studies of high index coatings were performed. In the first study, some common materials were tested (HfO_2, Sc_2O_3, and Ta_2O_5) [16]. In the second study, HfO_2 films prepared by three different methods (ion-beam sputtering, electron-beam evaporation, and atomic layer deposition) were compared [17]. These were all tested with 10 ns pulses at 1064 nm.

Figure 6 shows the defect distributions for films of HfO_2, Sc_2O_3, and Ta_2O_5. In the case of HfO_2, films prepared by ion-beam sputtering (IBS) and electron-beam (EB) evaporation were tested. In all cases, there is a region indicated as 'dark'. This indicates that the defect density could not be estimated because no damage events occurred in this range of fluences. STEREO-LID is able to provide a rich picture of the defects in these films. Ta_2O_5 has a very high density of defects at low fluences which is why it is a poor material for high-intensity pulsed laser applications. HfO_2, which is the most common material for pulse laser optical coatings, has a much lower defect density. STEREO-LID is able to show that the IBS film has a slightly lower defect density at low fluences, probably due to the more energetic deposition process. Finally, STEREO-LID shows that Sc_2O_3 has the lowest defect density of all at low fluences and that a significant spike in defects is observed near 1.2 J/cm^2. This high fluence feature may indicate the onset of intrinsic damage. This feature is not observed in the other films, because the density of defects is so high that no events were observed at high fluences.

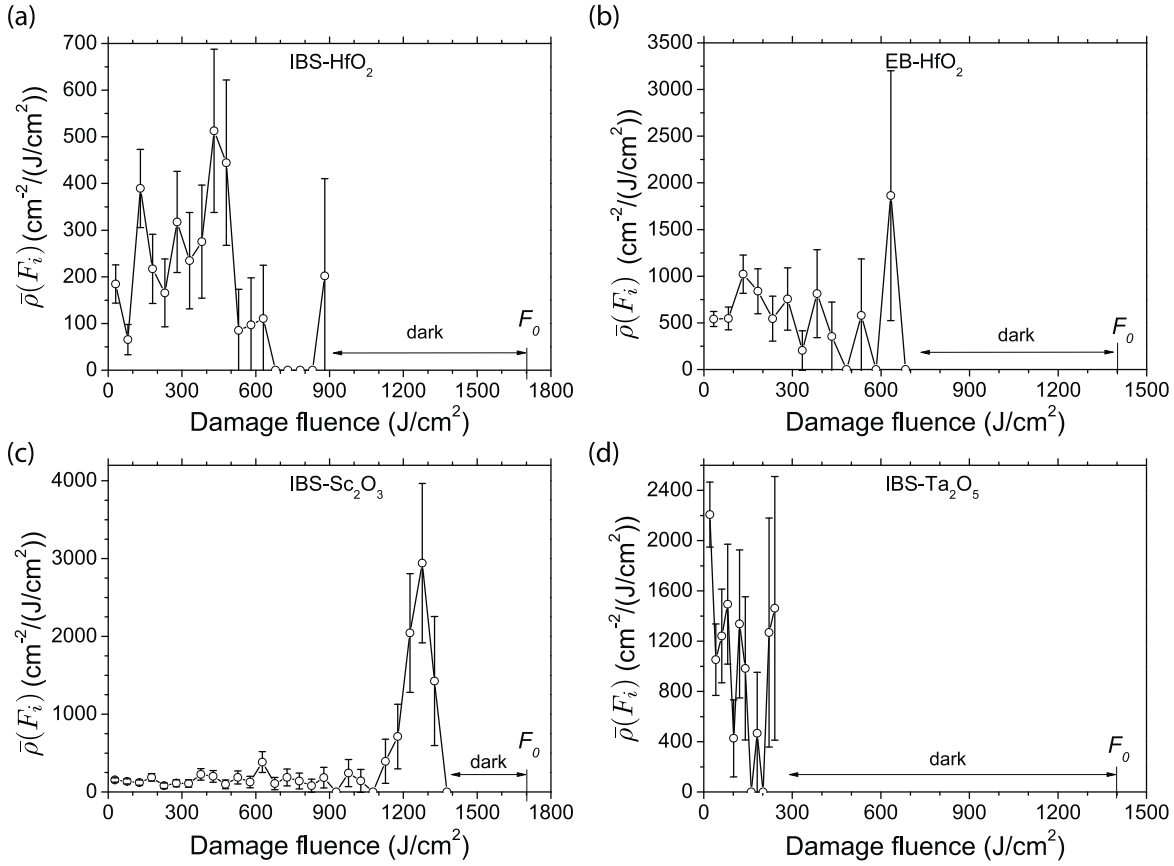

Figure 6: Defect density distribution functions retrieved from STEREO-LID characterization of four films: (a) IBS-HfO_2, (b) electron-beam HfO_2, (c) IBS-Sc_2O_3, and (d) IBS Ta_2O_5.

Figure 7 shows the result of the second tests performed on a set of 30 nm HfO_2 coatings prepared by IBS, EB, and atomic layer deposition (ALD). In addition data for a blank substrate is included to show that the defects in the substrate are not significant. The main result is that the difference between the IBS and EB films are even more dramatic for these very thin films. The quality of IBS films is known to degrade as the films get thicker. This clearly shows that the initial IBS films has defect densities on the order of the substrate at low fluences. The other observation is that the ALD film had very high defect densities, even higher than the EB film. This was surprising as ALD films are used in microelectronics because of their low defect densities. However, this was attributed to contamination in the ALD system. High speed ALD [19] is promising for multilayers because the inherent atomic-scale thickness control.

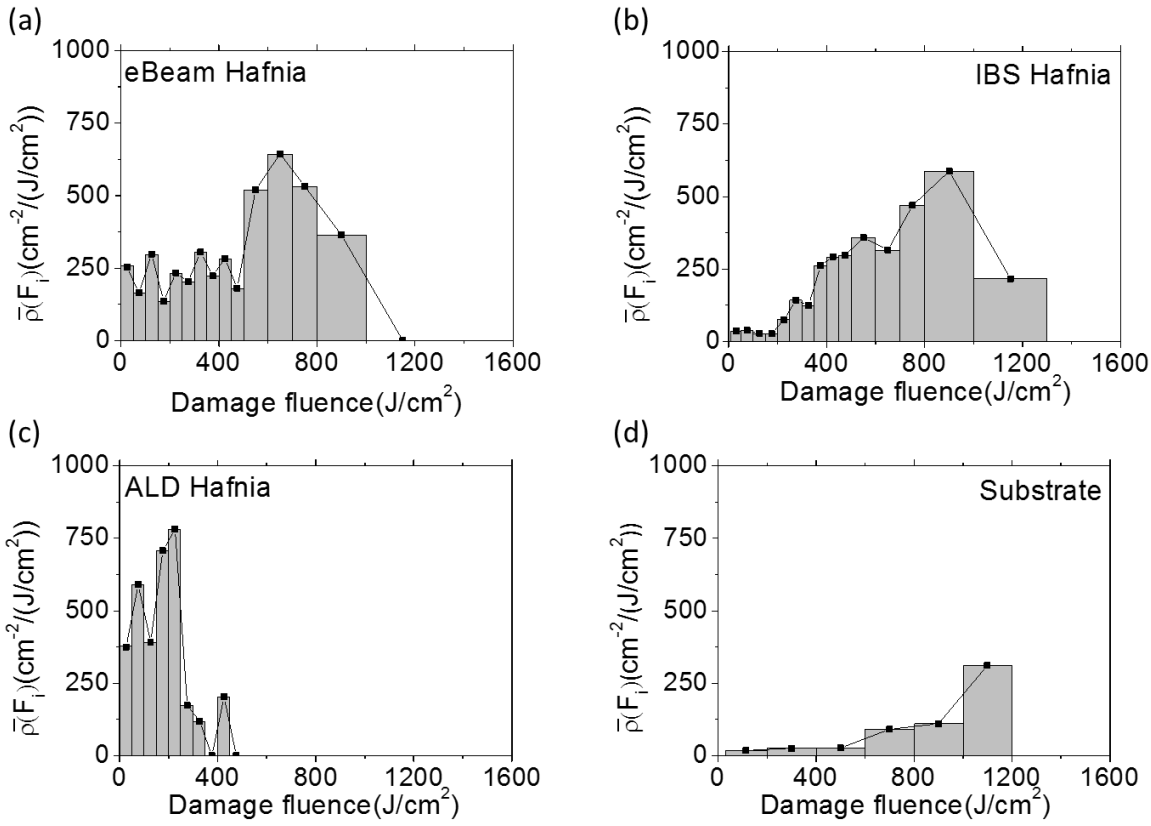

Figure 7: The retrieved defect density distributions $\bar{\rho}(F)$ for 30 nm HfO_2 films prepared by (a) electron beam evaporation, (b) ion-beam sputtering, and (c) atomic layer deposition (ALD). The defect density of a bare substrate (d) was also taken to show that the defects resulted primarily from the overcoated films.

3.3. Initial kinetics of damage growth following defect-initiated damage

As part of the STEREO-LID measurement, damage initiation is monitored through changes in transmission of an optical part. It has been found that transmission of a beam focused to 20

microns can be blocked in as little as 1 nanosecond. The implication is that the damage in the optic grows from some nanometer scale defect to many microns in size. Thus, the expansion spees of the absorption front exceeds the speed of sound. The processes that determine this growth are important as they determine the extent of damage (e.g. size of resultant crater) which is important in limiting damage in operational systems.

Figure 8 illustrates the process by which damage occurs [20]. Damage is initiated by absorption at a localized coating defect. This defect heats to the point where the overheated, high-pressure plasma is ejected in the form of a jet. This event triggers the growth of an expanding opaque region that blocks the beam and cuts off the transmission. The opaque region is caused by ionization of the optical coating and the formation of a plasma. The expansion of this absorption region is driven by the absorption itself. The rate of expansion is a function of the local laser intensity at the edge of the absorbing region, i.e. $v(F)$. The process has similarities to the expansion of an explosion front. The source of energy here is a chemical reaction, in our case the absorption of laser radiation.

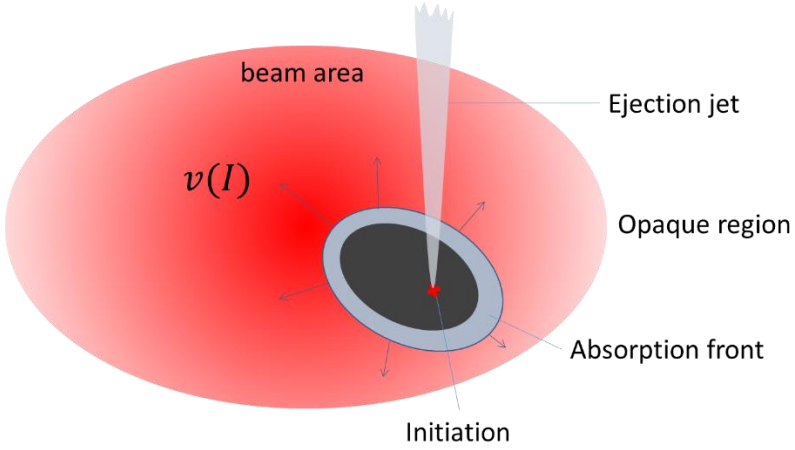

Figure 8: Model of laser-induced damage growth. An opaque absorption region grows out from the initiation point following ablation of the defect at a velocity that is proportional to the local intensity.

Figure 9 shows simulated transmission on real data using this phenomenological model. To fit the data, the model predicts that the local velocity is proportional to the square root of the local intensity,

$$v \propto I^{1/2} \tag{3}$$

The model can fit data for small beams (Fig. 9a) and large beam (Fig. 9b), where the size of the crater is limited by the growth of this expanding opaque region. In the case of a large beam, the predicted size of the opaque region underestimates the size the resultant crater by as much as 50%. We conclude that the size of the crater is determined by additional processes that follow the laser pulse.

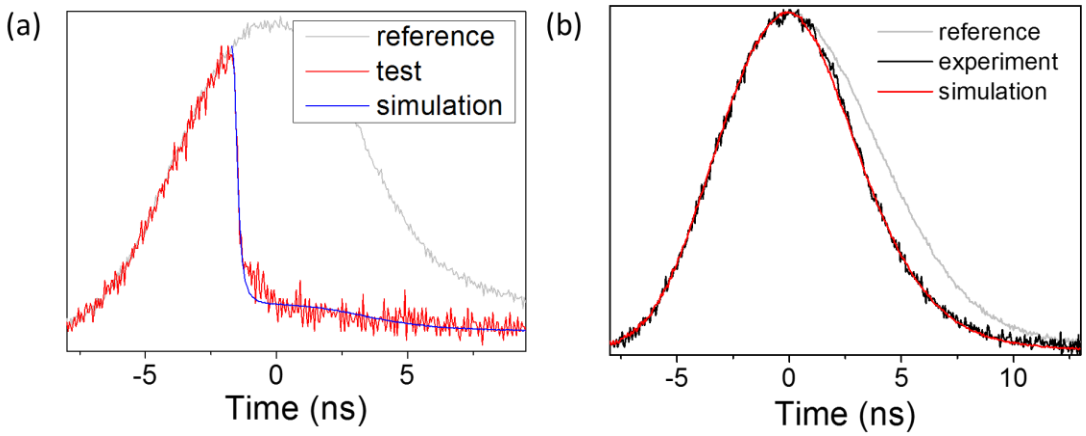

Figure 9: Example transmission data with fit using model with expansion using eqn. (3). (a) 22 µm beam and (b) 130 µm beam.

The dependence of expansion rate velocity on the square root of the intensity can be explained by a detonation wave [21]. The compression and heating from the front end of the wave initiates the generation of a plasma and the absorption of the back end of the wave propels the wave forward.

In summary, with STEREO-LID a technique is available for the first time that can measure the laser-induced damage threshold fluence (intensity) of an optical coating or surface in a single test. There are proposals under review to include this method in the new ISO standards for material inspection for high-power laser radiation. STEREO-LID has the following advantages over the existing ISO standards:

1. STEREO-LID can reproduce all the results of the ISO damage protocol with fewer overall tests.
2. Because it measures the actual damage fluence (intensity) it provides more information about the damage process than the ISO method based on recording of damage events and statistics.
3. Finally, STEREO-LID data can be used to retrieve the defect distribution without a priori assumptions about its functional form

4. Third harmonic generation in optical coatings

2.1 Third harmonic imaging of anisotropy

The third harmonic (TH) microscope is a scanning microscope in the sample is illuminated with a train of laser pulses and the image is generated by detecting the third harmonic light generated within the focus of the microscope. Figure 10 shows the experimental setup of our

TH microscope and illumination laser. The laser delivers 60-fs pulses at 100 MHz and 800 nm at an average power of up to 1 W. The third harmonic generated at 266 nm.

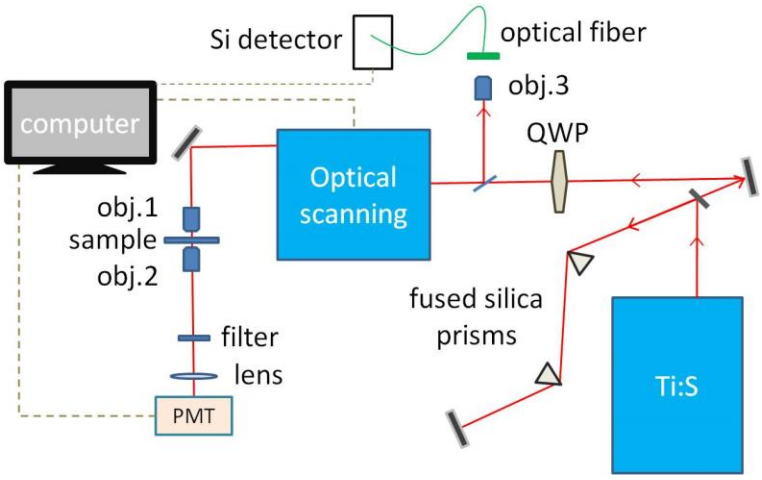

Figure 10: Schematic diagram of the third-harmonic microscope and illumination laser. The beam is focused onto the sample and raster-scanned. The generated third-harmonic power is the image signal, which is displayed on a computer. The computer also controls the x,y galvano scanners.

Using a quarter-wave plate, the microscope illumination was operated in two modes: linear and circular polarization. For isotropic materials, third harmonic in circular polarization (THCP) goes to zero due to symmetry. Therefore, any signal observed is an indicator of anisotropy resulting from intrinsic or induced defects. The following are highlights exploring the use of THCP to study anisotropic defects (both laser-induced and intrinsic) in various oxide films. The highlights are:

1. Demonstration of high-dynamic contrast using laser-induced damage crater.
2. Sensitivity to near damage threshold laser-induced material modifications that were not visible with other microscopies.
3. Demonstration of signal generated within the strain field around nano-indented material.
4. Observation of structures in as-grown films at the detection limit and their correlation with macro-strain.

High-dynamic contrast of third harmonic microscopy

A huge dynamic contrast is demonstrated in third harmonic microscopy for laser-induced damage. This feature results from the low background of the third harmonic signal for an amorphous film. Figure 11 shows the third harmonic image of a laser-induced damage crater in a dielectric film for different values of the detector gain.

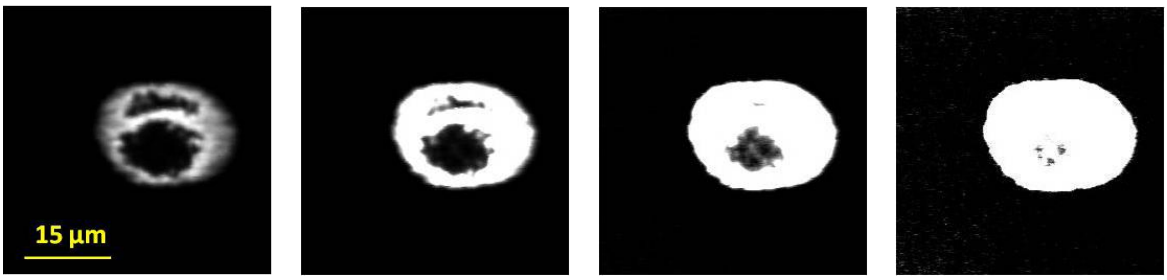

(a) (b) (c) (d)

Figure 11: (a)-(d) THCP images of a laser-induced damage crater with increasing gain on the PMT detector to capture signals across the total dynamic range. From left to right the gain increases by a total factor of ~ 200.

The dynamic contrast is the ratio of the strongest signal to the strength of background signal. From this series of images, we extract a value of 10^6:1. A comparison to other linear optical techniques using the same damage crater is shown in Table 1. In a distant second is Dark Field microscopy, another technique with a low background signal.

Table 1: Comparison of dynamic contrast for damage crater in Fig. 9.

Imaging Technique	Bright Field	Nomarski	Polarization Contrast	Dark Field	THCP
Dynamic range	5:1	6:1	7:1	756:1	10^6:1

Sensitivity to Laser-Induced Modifications

The low background of THCP images also makes it very sensitive to minor laser-induced modifications. The standard technique for identifying laser-induced damage is Nomarski microscopy. Figure 12 shows images of a laser-induced change in a HfO_2 film created by a train of subps laser pulses near the damage threshold. A subtle change is observed in Nomarski just above the noise level and only pops out in the line scan (Fig. 12c). The same spot in THCP shows a spot with a signal-to-noise ratio of nearly 200. Thus THCP has the potential to identify weaknesses in optics *in situ* before failure.

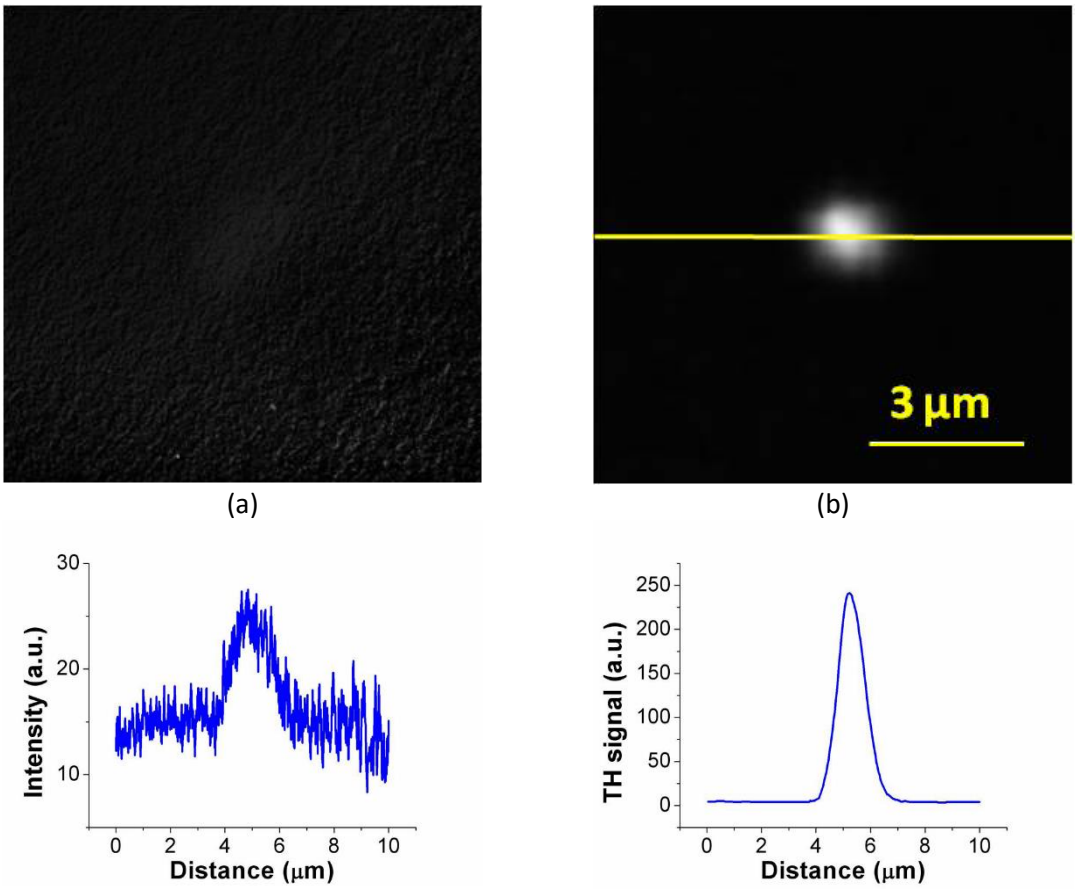

Figure 12: Comparison of (a) Nomarski and (b) THCP images of a laser-induced modification in a dielectric film. (c) and (d) are line scans to illustrate the difference in signal-to-noise ratio.

Stress field around nano-indentation

Figure 13 demonstrates the sensitivity of THCP to local stresses. A nanoindentation was prepared into the surface of fused silica by loading a pyramidal indenter past the plastic limit. The three images are THCP, THLP, and a darkfield image. The THCP image exhibits three lobes around the indentation that we attribute to plastically deformed material. Such lobes have been demonstrated by Raman microscopy [4].

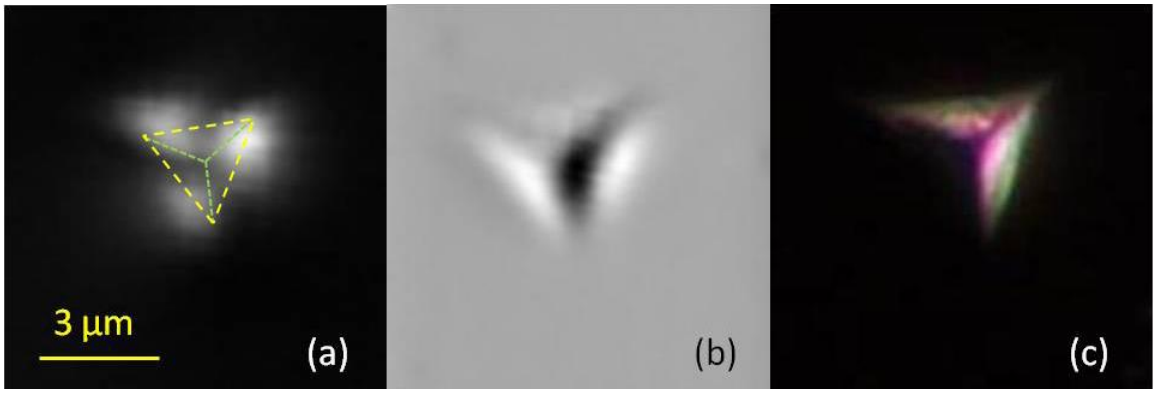

Figure 13: (a) THCP, (b) THLP, and (c) dark field images of the same 100 mN nanoindentation. The overlaid triangle indicates the relative outline of the THLP image.

Third Harmonic contrast from as-grown films.

Figure 14 shows THCP images of two as-grown Sc_2O_3 films taken at the detection limit of the system. What appears to be noise is reproducible diffraction limited features of the film. Real noise in this system appears as individual pixels (subdiffraction) that change from image to image.

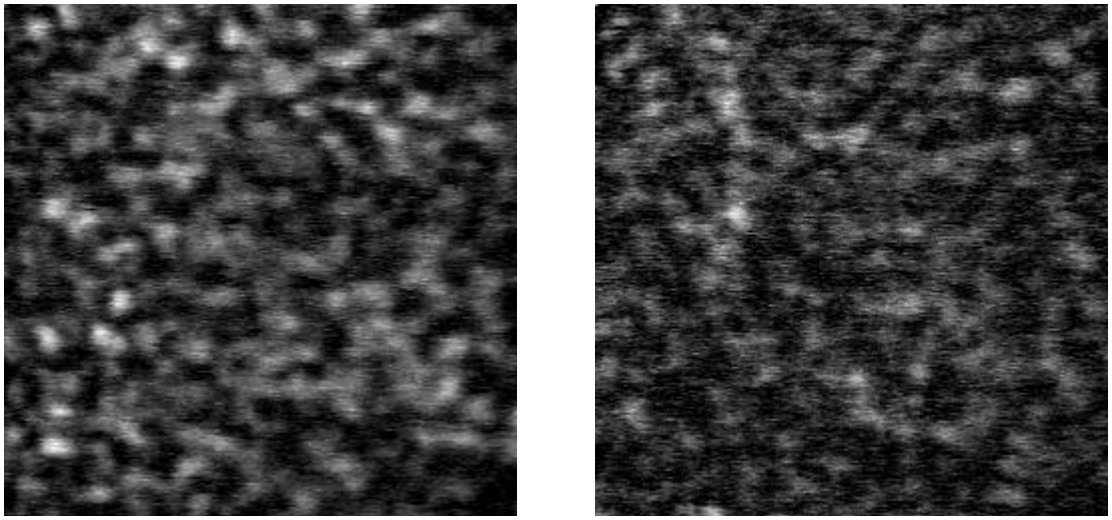

(a) (b)

Figure 14: THCP images of two Sc_2O_3 films (both 206 nm) taken at the detection limit. Average of 10 images with the background removed.

We characterized these features by their RMS about their average for three films and compared other measurements of these films such as surface roughness, x-ray diffraction intensity, and absorption. The strongest correlation was to the measured macro-stress in the films. These features may correspond to fluctuations in the local strain which can break the isotropic symmetry in the film.

4.2. Third harmonic generation in stacks of films

As part of the characterization of the third harmonic microscope, a model for predicting third harmonic generation in single layers and stacks was developed [22] and first tests of a prototype sample performed. While this was not part of the original project plan the first succesul steps in this direction were well worth it since it opened a whole new area for coating development – nonlinear optics with interference coatings

As input for this model, the nonlinear optical constants of many optical coatings were measured [23]. These were found to scale with the bandgap, E_g, of the material according to

$$\chi^{(3)} \propto (E_g^2 - E_3^2 - i\gamma E_3)^{-1}, \qquad (4)$$

where γ is a damping parameter and $E_3 = 3h\nu$ is the photon energy of the third harmonic. The data and this scaling are shown in Fig. 15.

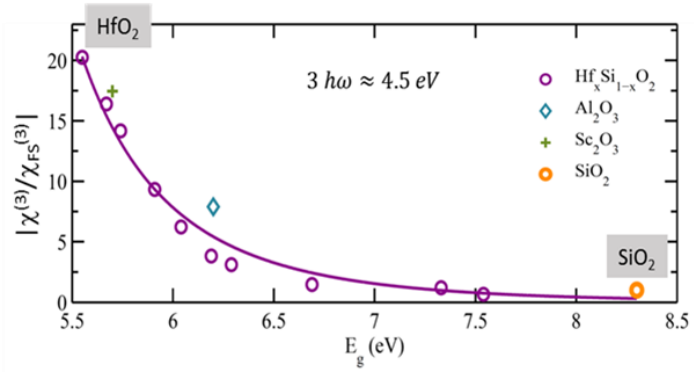

Figure 15: *Measured $|\chi^{(3)}|^2$ for THG of various metal oxide films (ion-beam sputtered) normalized to fused silica (FS). The solid line is a fit to Eq. (4) [23]. Varying x for the binary oxide $Hf_xSi_{1-x}O_2$ allowed us to change the bandgap energy [23]. Test wavelength: 800 nm.*

The model for third harmonic generation in a stack of layers was then used to design a mirror optimized to generate third harmonic in reflection. Such a mirror could be used to replace expensive crystals in many applications. A demonstration of the proof-of-concept mirror in shown in Fig. 16.

a) 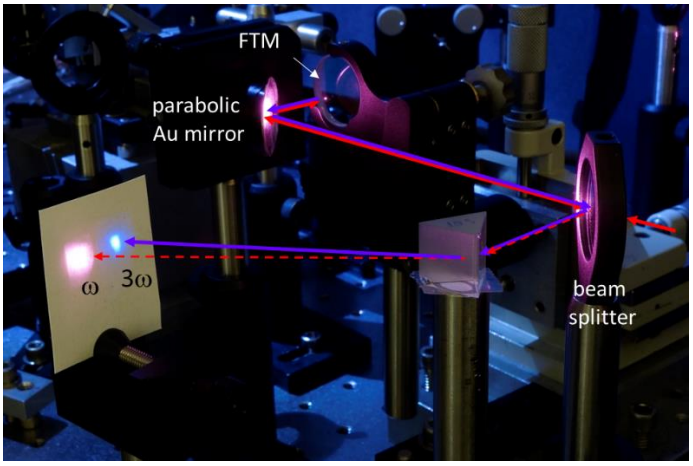

(b) 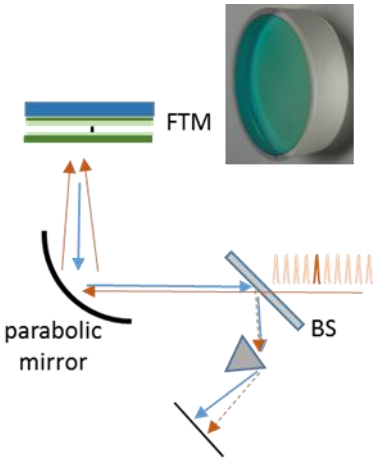

*Figure 16***:** *Recent proof-of-concept demonstration of third-harmonic generation using a frequency tripling mirror (FTM) in our lab [8]. (a) Photo of the FTM demonstration showing fluorescence from a white card excited by the 3ω (UV) beam (laser source: 800 nm, 55 fs, 100 MHz repetition rate train or bursts of pulses). (b) Schematic diagram of the experimental setup and photo of the FTM. Single-pulse conversion efficiencies approaching one percent have been observed.*

Summary

The highlights for the reporting period (11/1/10-9/31/16) include the following:

1. Study of the point defects in optimized Sc_2O_3 optical coatings.
2. Demonstration of improved laser damage resistance in functional mirrors by modifications to the top layer design.
3. Development of a new damage testing method (STEREO-LID) that is able to measure the laser-induced damage threshold of defects in optical coatings and surfaces.
4. Study of third harmonic generation in optical coatings for the characterization of defects and a mirror optimized for third harmonic generation as a first demonstration of nonlinear optics in optical coatings.

References

1. C. S. Menoni, P. F. Langston, E. Krous, D. Patel, L. A. Emmert, A. Markosyan, B. Reagan, K. Wernsing, R. Route, M. M. Fejer, J. J. Rocca, and W. Rudolph, “What role do point defects play in the laser damage behavior of metal oxides?” Proc. SPIE **8530**, 85300J (2012).
2. P. F. Langston, E. Krous, D. Schiltz, D. Patel, L. Emmert, A. Markosyan, B. Reagan, K. Wernsing, Y. Xu, Z. Sun, R. Route, M. Fejer, J. Rocca, W. Rudolph, and C. S. Menoni, "Point Defects in Sc_2O_3 Thin Films by Ion Beam Sputtering," in *Optical Interference Coatings*, M. Tilsch and D. Ristau, eds., OSA Technical Digest (online) (Optical Society of America, 2013), paper ThB.1. http://www.opticsinfobase.org/abstract.cfm?URI=OIC-2013-ThB.1

3. P. F. Langston, E. Krous, D. Schiltz, D. Patel, L. Emmert, A. Markosyan, B. Reagan, K. Wernsing, Y. Xu, Z. Sun, R. Route, M. Fejer, J. Rocca, W. Rudolph, and C.S. Menoni**,** "Point defects in Sc_2O_3 thin films by ion beam sputtering," Applied Optics **53**, A276-A280 (2014).
4. D. Patel, P. F. Langston, L. M. Imbler, L. A. Emmert, W. Rudolph, A. S. Markosyan, R. Route, M. M. Fejer, and C. S. Menoni, "Optimization of ion beam sputtered Y_2O_3 for high laser damage resistance," Proc. SPIE 8530, 85300Z (2012).
5. D. Patel, Drew D. Schiltz, P. Langton, L. A. Emmert, L. Acquaroli, C. Baumgarten, B. A. Reagan, J. J. Rocca, W. Rudolph, A. S. Markosyan, R. Route, M. M. Fejer, C. S. Menoni, "Improvements in the laser damage behavior of Ta_2O_5/SiO_2 interference coatings by modification of the top layer design", Proc. SPIE 8885, 888522 (2013).
6. D. Schiltz, D. Patel, L. A. Emmert, C. Baumgarten, B. Reagan, W. Rudolph, J. J. Rocca, and C. S. Menoni, "Modification of multilayer mirror top-layer design for increased laser damage resistance," Proc. SPIE 9237, 92371G (2014).
7. D. Schilz, D. Patel, C. Baumgarten, B. A. Reagan, J. J. Rocca, and C. S. Menoni, "Strategies to increase laser damage performance of Ta_2O_5/SiO_2 mirrors by modifications of the top layer design," Appl. Opt. 56, pp. C136-C139 (2017).
8. C. Rodriguez, S. Günster, D. Ristau, and W. Rudolph, "Frequency tripling mirror," Opt. Express **23**, pp. 31594-31598 (2015).
9. Z. Sun, M. Lenzner, and W. Rudolph, "Generic incubation law for laser damage and ablation thresholds," J. Appl. Phys. **117**, 073102 (2015).
10. Z. Sun, L. A. Emmert, X. Zhang, A. Mansoori, D. Patel, C. S. Menoni, and W. Rudolph, "Confocal photothermal microscopy of thin films based on etalon and thermal lensing effects," Proc. SPIE 8885, 888572 (2013).
11. X. Zhang , L. A. Emmert, and W. Rudolph, "Time-dependent absorption of TiO_2 optical thin films under pulsed and CW 800 nm laser irradiation," Appl. Opt. 52, pp. 8245-8251 (2013).
12. 1. E. Jankowska, S. Drobczynski, and C. S. Menoni, "Analysis of surface deformation in thin-film coatings by carrier frequency interferometry," Appl. Opt. **56**, pp. C60-C64 (2017).
13. R. A. Weber, C. Rodriguez, D. N. Nguyen, L. A. Emmert, D. Patel, C. S. Menoni, and W. Rudolph, "Third harmonic microscopy of intrinsic and induced material anisotropy in dielectric thin films," Opt. Eng. 51(12), 121807 (2012).
14. Y. Xu, L. A. Emmert, and W. Rudolph, "Spatio-TEmporally REsolved Optical Laser Induced Damage (STEREO LID) technique for material characterization," Opt. Express **23**, pp. 21607-21614 (2015).
15. Y. Xu, L. A. Emmert, and W. Rudolph, "Determination of defect densities from spatiotemporally resolved optical-laser induced damage measurements," Appl. Opt. **54**, pp. 6813-6819 (2015).
16. Y. Xu, M. R. Abdulameer, L. A. Emmert, T. Day, D. Patel, C. S. Menoni, and W. Rudolph, "Comparison of defects responsible for nanosecond laser-induced damage and ablation in common high index optical coatings," Opt. Eng. 56, 011019 (2017).
17. Y. Xu, A. Khabbazi Oskouei, T. Day, A. Brown, L. A. Emmert, J. J. Talghader, E. Field, D. Kletecka, J. Bellum, D. Patel, C. S. Menoni, and W. Rudolph, "Comparative STEREO-

LID (Spatio-TEmporally REsolved Optical Laser-Induced Damage) studies of critical defect distributions in IBS, ALD, and electron-beam coated dielectric films," Proc. SPIE 9632, 963215 (2015).
18. A. S. Foster, F. L. Gejo, A. L. Shluger, and R. M. Nieminen, "Vacancy and interstitial defects in hafnia," Phys. Rev. B **65**, 174117 (2002).
19. P. Poodt, A. Lankhorst, F. Roozeboom, K. Spee, D. Maas, and A. Vermeer, "High-Speed Spatial Atomic-Layer Deposition of Aluminum Oxide Layers for Solar Cell Passivation," Advanced Materials **22**, pp. 3564-3567 (2010).
20. Y. Xu, L. A. Emmert, T. Day, D. Patel, C. S. Menoni, D. Dunlap, and W. Rudolph, manuscript in preparation.
21. D. L. Chapman, Phil. Mag. 47, pp. 90-104 (1899)
22. C. Rodriguez and W. Rudolph, "Modeling third-harmonic generation from layered materials using nonlinear optical matrices", Opt. Express **22**, pp. 25984-92 (2014).
23. C. Rodriguez and W. Rudolph, "Characterization and $\chi^{(3)}$ measurements of thin films by third-harmonic microscopy", Opt. Lett. **39**, pp. 6042-45 (2014).